

High density adsorbed oxygen on Rh(111) and enhanced routes to metallic oxidation using atomic oxygen

K. D. Gibson, Mark Viste, Errol C. Sanchez, and S. J. Sibener

The James Franck Institute and The Department of Chemistry, The University of Chicago, Chicago, Illinois 60637

(Received 4 November 1998; accepted 30 November 1998)

Exposure of Rh(111) to atomic oxygen leads to the facile formation of a full-coverage and ordered (1×1) -O monolayer which is stable at room temperature. This result differs markedly from the half-coverage (2×1) -O overlayer which forms at saturation when using molecular oxygen. This demonstrates that kinetic rather than thermodynamic constraints inhibit the formation of dense oxygen overlayers when O_2 is the oxidant. We also report that O absorption into the bulk proceeds much more readily when using O rather than O_2 , a finding with direct implications for enhanced methods of low-temperature metallic oxidation. These results demonstrate that there are important fundamental differences in the way in which low-energy beams of atomic and molecular oxygen interact with metals. © 1999 American Institute of Physics. [S0021-9606(99)71406-6]

One of the goals of modern surface science is to understand at the most fundamental level how oxygen interacts with metallic surfaces. This topic is of great technological importance due to the central role that oxygen-surface interactions have in determining the atomic-level mechanisms of such phenomena as metallic oxidation, corrosion, and chemical catalysis. To date, activity in this area of investigation has primarily concentrated on the interactions of molecular oxygen. We have recently initiated ultra-high-vacuum (UHV) gas-surface scattering experiments in which a beam of atomic oxygen interacts with various metallic interfaces, in this instance Rh(111). This allows us to examine oxygen-metal surface chemistry in which the constraint of starting with a molecular rather than an atomic oxidant has been lifted, and to elucidate whether differences exist in the rate of oxygen incorporation into the bulk depending on the nature of the oxidant, with concomitant consequences for metallic oxidation.

Much is already known about the adsorption and absorption of O on Rh(111).¹⁻³ Under UHV conditions, it is generally accepted that the saturation coverage for chemisorbed O originating from O_2 dosing is 0.5 monolayers (ML) (Refs. 4-8) (though a recent STM study,^{9,10} refuted by Ref. 8, claimed a saturation coverage of 0.25 ML). The formation of this half-coverage overlayer at a saturation exposure of O_2 is characteristic of other closest-packed transition metal surfaces as well. However, exceptions do exist when surface defects are present, or when other molecular oxidants are used which do not need to simultaneously deposit two chemisorbed oxygen atoms. For example, Parrott *et al.*¹¹ were able to grow 1 ML of adsorbed O on a stepped Ru crystal after long exposure to 10^{-5} Torr of O_2 at a surface temperature of 300 K. Moreover, NO_2 can produce high O coverages on the low-index planes of several transition metals including Pt(111),¹² Pd(111),¹³ and Ru(0001).¹⁴⁻¹⁶ Recently, an ordered (1×1) -O monolayer has been grown with NO_2 at 600 K on Ru(0001),¹⁶ as was suggested

theoretically.¹⁷ In addition to structural and chemisorption issues, further motivations for these studies comes from heterogeneous reaction studies involving O adsorbed on Ru(0001) (Refs. 18-20) and Rh(111),⁴ including new beam studies from our group²¹ which suggest large changes in catalytic activity and reaction mechanism with differing oxygen coverage.

The main thrust of this Communication will be to examine the interaction of an atomic oxygen beam with Rh(111). We will show this to be an effective way of producing a well-ordered (1×1) monolayer of O on Rh(111), as well as an efficient method of incorporating O into the bulk of the material. These results strongly imply that kinetic (dynamical) constraints associated with the dissociative chemisorption of O_2 at coverages above 0.5 ML rather than thermodynamic issues govern the formation of such high O-covered surfaces, a view recently confirmed by electronic structure calculations on this system.²² We have also been able to produce a well-ordered (1×1) -O overlayer on Rh(111) using NO_2 , to be discussed elsewhere.²¹

These experiments were performed in a unique three-supersonic-beam UHV gas-surface scattering instrument,^{23,24} only the essential features will be mentioned here. The three beams are generated in a quadruply-differentially pumped source chamber. These beams converge on the target crystal in the scattering chamber with base pressure $\sim 1 \times 10^{-10}$ Torr. Scattered neutral particles are detected with a doubly-differentially pumped quadrupole mass spectrometer (angular resolution $\sim 1^\circ$) which rotates around the position of the crystal. This rotation, which includes the surface normal, defines the plane in which we can detect scattered atoms.

The helium diffraction measurements were performed with a liquid nitrogen cooled source located in the center beam position. This produced a highly collimated He beam [$\langle E \rangle \cong 20$ meV; $\Delta v(\text{FWHM})/v \cong 1\%$]. The atomic oxygen beam was produced using a radio frequency discharge nozzle beam source²⁵ operated at 13.5 MHz, with a 1 mm diam

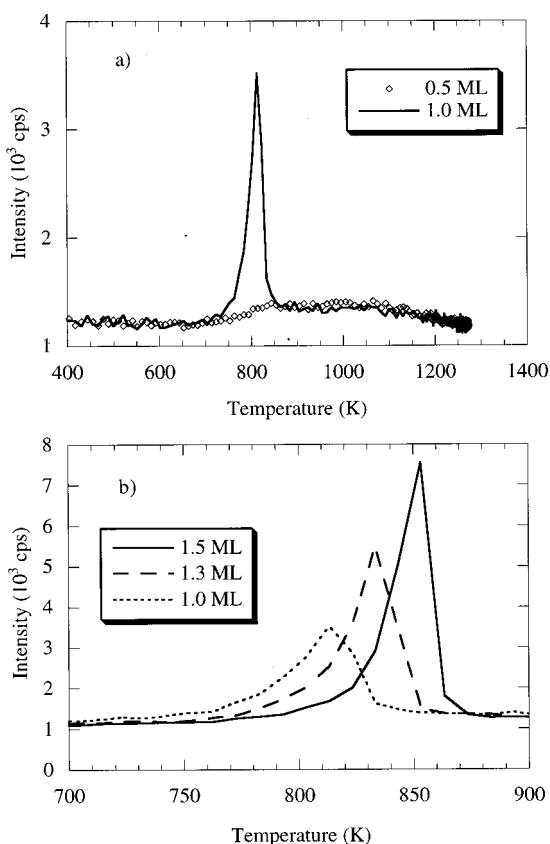


FIG. 1. Temperature programmed desorption spectra of O₂ desorbing from Rh(111) using a ramp rate of 10 K/s. (a) Comparison of TPD spectra following dosing with O₂ (open circles) and O (solid line). (b) TPD spectra for extended dosing with atomic oxygen. See text for further details.

nozzle, and a stagnation pressure between 1 and 4 Torr of O₂. The O number density fraction in the beam was determined to be ~30%.^{25–27} The beam was mildly supersonic, with the O₂ having an average energy of 80–90 meV, and the O having an average energy of about 60 meV. Depending upon the stagnation pressure, the total flux could be varied from 0.01 to 0.15 ML/s (1 ML = 1.6 × 10¹⁵ atoms/cm²).

The rhodium crystal was cut to within 1° of the (111) face, as confirmed by Laue x-ray diffraction. Crystal cleanliness was confirmed using Auger electron spectroscopy, and by monitoring the intensity and width of specularly reflected He. Coverage measurements were done using temperature programmed desorption (TPD), where the mass 32 signal of desorbing O₂ was monitored while ramping the crystal temperature. For calibration, we referenced a given experiment's TPD intensity to that for an O₂ dosed surface, which has a known saturation coverage of $\Theta_{O_2} = 0.5$ ML.

Figure 1 shows O₂ TPD spectra taken using a ramp rate of 10 K/s for varying amounts of oxygen deposited at $T_S = 325$ K. In Fig. 1(a), the open circles are the O₂ dosed "reference" TPD spectrum where the total amount of O₂ desorbed is 0.5 ML. Here the O₂ desorbs over a temperature range from about 700 K to greater than 1200 K. At this surface temperature, continued dosing with O₂ does not result in a measurable increase in the amount of desorbed O₂. The other TPD data set of Fig. 1(a) has an integrated inten-

sity twice that of the O₂ dosed surface, i.e., $\Theta_{O_2} = 1.0$ ML. This oxygen coverage corresponds to the minimum amount that is needed to completely convert the surface structure from a (2×1)-O to a (1×1)-O overlayer, confirming the formation of a 100% O-covered surface. The TPD data of Fig. 1(b) reveal that even higher coverages than 1 ML of oxygen can be easily generated when dosing with atomic oxygen; the TPD spectra have features that can be clearly associated with both ad- and absorbed oxygen.²⁸ The O₂ in excess of 0.5 ML desorbs as a narrow peak at ~800–850 K, with the peak temperature shifting upwards with greater quantities of O₂.

Figure 2 presents a detailed comparison of He diffraction data ($T_S = 325$ K) along two principal symmetry directions for Rh(111) dosed with either molecular or atomic oxygen. The diffraction data of Figs. 2(a) and 2(c), corresponding to dosing with molecular oxygen, are characteristic of the 0.5 ML covered surface which consists of multiple (2×1) domains which have their axes oriented along different symmetry directions, giving a net (2×2) diffraction pattern. The characteristic half-order diffraction peaks for this structure are marked with arrows in these figures. The diffraction data for the atomic oxygen dosed surface, Figs. 2(b) and 2(d), differ markedly from the molecular oxygen dosed data. Most notably, the half-order diffraction peaks characteristic of the (2×1) overlayer have essentially disappeared for the 1.0 ML O-covered surface. *The angular positions of the principle diffraction features are consistent with a commensurate (1×1)-O/Rh(111) overlayer (Rh–Rh distance = 2.69 Å).* A very small residual half-order peak in the $\langle 10\bar{1} \rangle$ direction can be seen in Fig. 2(d); this may be due to a slight adsorbate-induced buckling of the Rh(111) surface, not uncommon for close-packed metal surfaces.²⁹

We have shown compelling He diffraction and TPD evidence that dosing with atomic oxygen leads to the facile formation of a (1×1)-O surface structure which has $\Theta_{O_2} = 1.0$ ML. This result differs from that obtained when using molecular oxygen, which leads to the formation of a (2×1)-O surface structure with $\Theta_{O_2} = 0.5$ ML. We can rule out the possibility that O₂ dosing leads to a saturated 0.25 ML structure; if this were the case, then O atom dosing would have deposited only 0.5 ML, yielding prominent higher-order features in the diffraction spectra—features not observed in our experiments. We also note that even though it is possible to deposit more than 0.5 ML of O with long O₂ exposure of the Rh(111) surface at elevated surface temperatures, that the associated diffraction spectra still show pronounced half-order peaks. This indicates that for O₂ dosing the extra oxygen is absorbed into the bulk, and does not reside at the surface.

Figure 3(a) shows the absorption isotherm for atomic oxygen at $T_S = 325$ K. The data points were obtained from TPD data. The solid line, which provides a quantitative fit to the data, assumes first-order Langmuir adsorption kinetics,

$$\frac{d\Theta_{O_2}}{dt} = S_0\Phi(1 - \Theta_{O_2}), \quad (1)$$

where Φ is the flux of O atoms and S_0 is the initial sticking coefficient. This first-order adsorption line was fit to the data

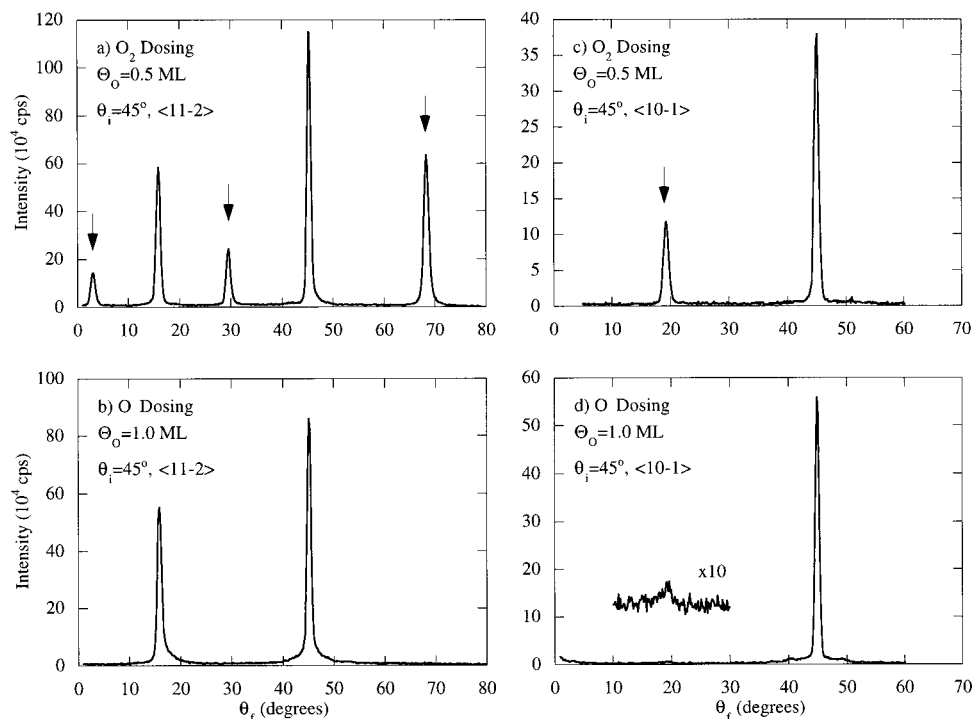


FIG. 2. He diffraction data taken along two principal symmetry directions which confirm that O_2 dosing at $T_S=325$ K [panels (a) and (c)] produces a (2×1) -O overlayer, while dosing with atomic oxygen [panels (b) and (d)] yields a (1×1) -O overlayer. Scattering conditions were $\theta_i=45^\circ$ and $T_S=325$ K for all data with $E_i=20$ meV along $\langle 11\bar{2} \rangle$ and 20.1 meV along $\langle 10\bar{1} \rangle$. Arrows in panels (a) and (c) indicate the positions of half-order peaks which do not appear for the O-dosed surface.

at coverages where O_2 adsorption does not occur, i.e., $\theta_O > 0.5$. Using the estimated O-flux, S_0 is found to be 0.3. The implication is that impinging atoms either find a vacancy or are reflected. O_2 behaves differently, with the dissociative adsorption isotherm following second-order kinetics;² this isotherm is represented by a dashed line in Fig. 3(a).

The absence of change in consecutive diffraction runs taken during a 30 min period indicates that the (1×1) -O overlayer is stable at $T_S=325$ K. To investigate the stability of the (1×1) -O overlayer at higher surface temperatures, we first grew 1.0 ML overlayers at $T_S=325$ K. Reference He diffraction data were taken, followed by heating to a specified elevated temperature for 5 min. Finally, the surface was cooled back to 325 K and a diffraction spectrum taken for comparison to the reference structure. Between 400 K and 425 K, small half-order peaks appeared, indicating the depletion of surface oxygen. This trend becomes much more pronounced at 525 K, where half-order peaks become quite evident after heating for only 30 s. Most of the missing surface oxygen becomes absorbed at this temperature.

We now examine the facile absorption of oxygen into the bulk metal when dosing with atomic oxygen. It is possible, as shown in Fig. 1(b), to deposit more than 1.0 ML of oxygen when dosing with O. He diffraction experiments indicate that this occurs while still maintaining a well-ordered (1×1) -O overlayer. This provides clear evidence that we are not growing a compressed phase of adsorbed O, but rather that the extra O absorbs into the bulk. A comparison of the measured absorption rates for O vs O_2 is shown in Fig. 3(b). The rates for O_2 dosing have been previously measured for temperatures between 400 K and 600 K using a room temperature supersonic beam with a flux of 1 ML/s.¹ The solid line shown in Fig. 3(b) is a fit to these prior data, extrapolated to lower temperatures. At $T_S=325$ K, we were unable

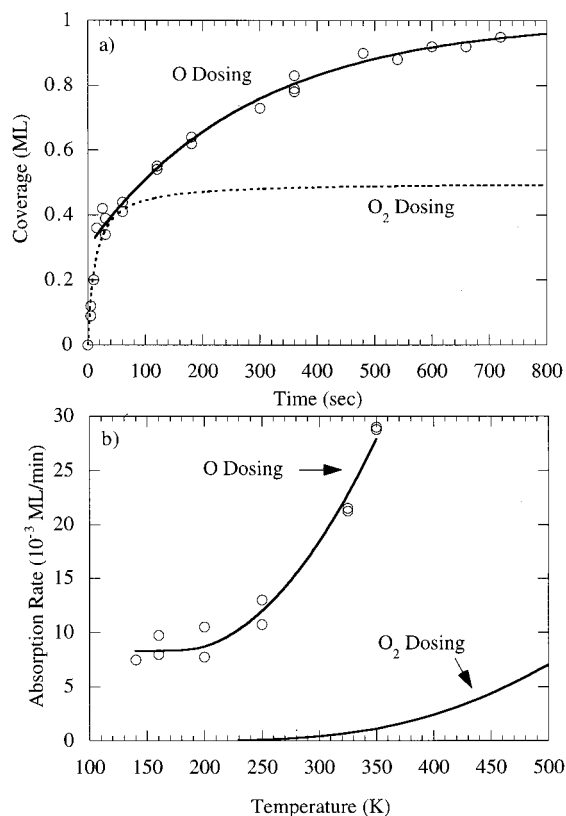


FIG. 3. (a) Adsorption isotherms at $T_S=325$ K for O_2 and O dosing which exhibit second-order and first-order Langmuir behavior, respectively. The open circles are the measured data for O-dosing, while the solid line is the fit for a first-order isotherm. Total oxygen flux was 0.038 ML/s with an O atom flux of 0.013 ML/s. The dashed line is a second-order isotherm for O_2 . (b) Comparison of oxygen absorption rates for dosing with O and O_2 as a function of substrate temperature. Total oxygen flux for the O dosing experiment was 0.046 ML/s with an O atom flux of 0.017 ML/s. The O_2 curve is from the data of Peterlinz *et al.* (Ref. 1), with an O_2 flux of 1 ML/s.

to measure any additional oxygen uptake with as much as 80 min of O₂ exposure after the completion of 0.5 ML coverage. The circles in Fig. 3(b) are the measured rates for oxygen absorption when dosing with the O atom beam using conditions which maintained the ordered (1×1)-O overlayer. These results indicate a dramatic enhancement in the rate of oxygen incorporation into the bulk when exposing the substrate to atomic oxygen, a finding with important consequences for low-temperature metallic oxidation and materials degradation.

To summarize, we have demonstrated that the Rh(111) surface is capable of supporting a full monolayer of adsorbed O when using atomic O for dosing. It is adsorbed as a well-ordered (1×1)-O overlayer, as shown by He atom diffraction. The facile formation of a stable (1×1)-O/Rh(111) structure when dosing with atomic oxygen stands in sharp contrast to the limiting value of 0.5 ML which is reached when dosing with molecular oxygen. These findings emphasize that the dynamical path taken by oxygen molecules as they dissociatively chemisorb on metallic surfaces is critically influenced by adsorbate coverage. This strongly suggests that for dissociative adsorption to occur a relatively low-energy path must exist which accesses two adjacent surface sites. These pathways become energetically unfavorable and hence inaccessible for $\Theta_O > 0.5$ ML. Electronic structure calculations²² confirm this conclusion. Our observation that O absorption into the bulk proceeds much more readily when using O rather than O₂ is a finding with direct implications for low-temperature metallic oxidation. This suggests that the potential energy surface that governs oxygen transport across the surface-to-selvedge interface must also be highly dependent on O coverage, with the energetic barrier for migration from the (1×1)-O overlayer to the bulk being substantially lower than from the (2×1)-O overlayer. These results demonstrate that there are important fundamental differences in the way in which low-energy beams of atomic and molecular oxygen interact with metals. These studies further reinforce the sense that a predictive knowledge of how atomic oxygen reacts with materials spanning the range from thermal to high energy is as yet incomplete. We are

presently expanding these studies of atomic oxygen-surface interactions to include other metallic and organic interfaces.

This work was supported by the Air Force Office of Scientific Research, and, in part, by the NSF-MRSEC Program at The University of Chicago, Award No. DMR-9808595.

- ¹K. A. Peterlinz and S. J. Sibener, *J. Phys. Chem.* **99**, 2817 (1995).
- ²K. A. Peterlinz and S. J. Sibener, *Surf. Sci.* **344**, L1239 (1995).
- ³P. A. Thiel, J. T. Yates, Jr., and W. H. Weinberg, *Surf. Sci.* **82**, 22 (1979).
- ⁴X. Xu and C. M. Friend, *J. Am. Chem. Soc.* **113**, 6779 (1991).
- ⁵C. T. Reimann, M. El-Maazawi, K. Walzl, B. J. Garrison, N. Winograd, and D. M. Deavon, *J. Chem. Phys.* **90**, 2027 (1989).
- ⁶K. C. Wong, W. Liu, and K. A. R. Mitchell, *Surf. Sci.* **360**, 137 (1996).
- ⁷S. Schwegmann, H. Over, V. De Renzi, and G. Ertl, *Surf. Sci.* **375**, 91 (1997).
- ⁸S. Schwegmann and H. Over, *Surf. Sci.* **393**, 179 (1997).
- ⁹H. Xu and K. Y. S. Ng, *Surf. Sci.* **375**, 161 (1997).
- ¹⁰H. Xu and K. Y. S. Ng, *Surf. Sci.* **393**, 181 (1997).
- ¹¹S. L. Parrott, G. Praline, B. E. Koel, J. M. White, and T. N. Taylor, *J. Chem. Phys.* **71**, 3352 (1979).
- ¹²D. H. Parker, M. E. Bartram, and B. E. Koel, *Surf. Sci.* **217**, 489 (1989).
- ¹³B. A. Banse and B. E. Koel, *Surf. Sci.* **232**, 275 (1990).
- ¹⁴I. J. Malik and J. Hrbek, *J. Vac. Sci. Technol. A* **10**, 2565 (1992).
- ¹⁵W. J. Mitchell and W. H. Weinberg, *J. Chem. Phys.* **104**, 9127 (1996).
- ¹⁶C. Stampfl, S. Schwegmann, H. Over, M. Scheffler, and G. Ertl, *Phys. Rev. Lett.* **77**, 3371 (1996).
- ¹⁷C. Stampfl and M. Scheffler, *Phys. Rev. B* **54**, 2868 (1996).
- ¹⁸C. H. F. Peden, in *Surface Science of Catalysis*, edited by D. J. Dwyer and F. M. Hoffmann (American Chemical Society, Washington, D.C., 1992).
- ¹⁹C. H. F. Peden, D. W. Goodman, M. D. Weisel, and F. M. Hoffmann, *Surf. Sci.* **253**, 44 (1991).
- ²⁰C. H. F. Peden and D. W. Goodman, *J. Phys. Chem.* **90**, 1360 (1986).
- ²¹K. D. Gibson, M. Viste, E. Sanchez, and S. J. Sibener (in preparation).
- ²²E. J. Walter, S. P. Lewis, and A. M. Rappe, *Phys. Rev. Lett.* (submitted).
- ²³D. F. Padowitz and S. J. Sibener, *Surf. Sci.* **254**, 125 (1991).
- ²⁴J. I. Colonell, K. D. Gibson, and S. J. Sibener, *J. Chem. Phys.* **103**, 6677 (1995).
- ²⁵S. J. Sibener, R. J. Buss, C. Y. Ng, and Y. T. Lee, *Rev. Sci. Instrum.* **51**, 167 (1980).
- ²⁶W. L. Fite and R. T. Brackmann, *Phys. Rev.* **113**, 815 (1959).
- ²⁷D. Rapp, P. Englander-Golden, and D. D. Briglia, *J. Chem. Phys.* **42**, 4081 (1965).
- ²⁸K. D. Gibson, J. I. Colonell, and S. J. Sibener, *Surf. Sci.* **343**, L1151 (1995).
- ²⁹U. Starke, M. A. Van Hove, and G. A. Somorjai, *Prog. Surf. Sci.* **46**, 305 (1994).